



Babeş-Bolyai University from Cluj-Napoca
Faculty of Chemistry and Chemical
Engineering



**RESEARCH AND DEVELOPMENT OF NEW
NANOMATERIALS BASED ON MAGNESIUM
SILICATES**

PhD Thesis summary

Scientific supervisor:
Prof.Dr. Maria Tomoaia-Cotisel

PhD student:
Marieta Adriana Naghiu

2013



Babeş-Bolyai University from Cluj-Napoca
Faculty of Chemistry and Chemical
Engineering



RESEARCH AND DEVELOPMENT OF NEW NANOMATERIALS BASED ON MAGNESIUM SILICATES

PhD Thesis summary

Jury:

President:

Prof. Dr. Eng. Mircea Dărăbanțu - “Babeş-Bolyai” University, Cluj-Napoca

Scientific supervisor:

Prof. Dr. Maria Tomoaia-Cotișel - “Babeş-Bolyai” University, Cluj-Napoca

Reviewers:

Prof. Dr. Minodora Leca - University from Bucharest

Prof. Dr. Elena Maria Pică - Technical University, Cluj-Napoca

Assoc. Prof. Dr. Eng. Maria Gorea – “Babeş-Bolyai” University, Cluj-Napoca

Public defence: September 20, 2013

TABLE OF CONTENTS:

Part I. Literature study

Introduction	2
1. Nanomaterials based on magnesium silicates	8
1.1. Nanomaterials.....	8
1.2. Sistem SiO ₂ -MgO.....	10
1.2.1. Forsterite (Mg ₂ SiO ₄)	12
1.2.2. Enstatite (MgSiO ₃)	16
1.3. Forsterite synthesis.....	17
1.3.1. Raw materials	17
1.3.1.1. Silicon based precursors.....	18
1.3.1.2. Magnesium based precursors	24
1.3.1.3. Additives.....	24
1.3.2. Preparation methods.....	25
1.3.2.1. Solid state reaction method.....	25
1.3.2.2. Sol-gel method.....	28
1.3.2.3. Precipitation method.....	31
2. Bioceramic materials	32
2.1. Overview.....	32
2.2. Obtaining of ceramics.....	36
2.3. Bioceramics based on magnesium silicates.....	40
2.3.1. Bioceramic based on enstatite.....	41
2.3.2. Bioceramic based on forsterite.....	41
References.....	43

Part II. Original contributions

3. Preparation of forsterite powder	56
3.1. Overview.....	56
3.1.1. Experimental compositions.....	57
3.1.2. Methods description.....	57
3.1.3. Powder characterization methods.....	58
3.2. Preparation of forsterite from colloidal silica	60
3.2.1. Compositions.....	61
3.2.2. Experimental procedures.....	61
3.2.3. Product characterization.....	63
3.2.3.1. Thermal behaviour of mixture.....	63
3.2.3.2. X-ray diffraction.....	63
3.2.3.3. FTIR Spectroscopy.....	64
3.2.3.4. SEM and AFM microscopy.....	67
Conclusions.....	68
3.3. Preparation of forsterite from TEOS.....	68
3.3.1. Preparation of forsterite by sol-gel methods from $Mg(NO_3)_2 \cdot 6H_2O$, TEOS and additives.....	68
3.3.1.1. Forsterite density.....	70
3.3.1.2. X-ray diffractometry.....	71
3.3.1.3. Particle size analysis.....	77
3.3.1.4. FTIR spectroscopy.....	73
3.3.1.5. AFM microscopy.....	73
3.3.1.6. SEM microscopy.....	75
3.3.1.7. In vitro bioactivity evaluation.....	78
3.3.1.7.1 FTIR spectroscopy.....	79
3.3.1.7.2 X-ray diffraction	80
3.3.1.7.3 Electron microscopy SEM +EDS.....	81
3.3.1.8. In vitro biocompatibility evaluation	82
3.3.1.8.1 Osteoblast cultures.....	82
3.3.1.8.2 Cytotoxicity test.....	85
3.3.1.9. Biocompatibility investigation on forsterite by optical	87

microscopy.....	95
Conclusions.....	95
3.3.2. Preparation of forsterite by sol-gel methods from $Mg(NO_3)_2 \cdot 6H_2O$ and TEOS, no additives.....	89
3.3.2.1. Thermal behavior of mixture.....	90
3.3.2.2. X-ray diffraction	93
3.3.2.3. Particle size analysis.....	94
3.3.3. Preparation of forsterite by precipitation method from $Mg(NO_3)_2 \cdot 6H_2O$ and TEOS.....	95
3.3.3.1. Thermal behavior of mixture.....	96
3.3.3.2. X-ray diffraction	98
3.3.3.3. Particle size analysis.....	99
3.3.3.4. Electron microscopy.....	99
Conclusions.....	100
3.4. Preparation of forsterite by solid state reaction methods from talc.....	101
3.4.1. Preparation of forsterite from $MgCO_3$ and talc	101
3.4.1.1. Thermal behavior of mixture.....	102
3.4.1.2. X-ray diffraction	104
3.4.1.3. Particle size analysis.....	105
3.4.1.4. AFM microscopy.....	106
3.4.1.5. TEM microscopy.....	107
3.4.1.6. SEM microscopy.....	108
3.4.1.7. In vitro bioactivity evaluation.....	109
Conclusions.....	110
3.4.2. Preparation of forsterite from $Mg(NO_3)_2 \cdot 6H_2O$ and talc.....	110
3.4.2.1. X-ray diffraction	111
3.4.2.2. Particle size analysis.....	112
3.4.2.3. AFM microscopy.....	112
3.4.2.4. SEM microscopy.....	114
Conclusions.....	116
3.4.3. Preparation of forsterite from $MgSO_4 \cdot 7H_2O$ and talc.....	116
3.4.3.1. X-ray diffraction	117
3.4.3.2. Particle size analysis.....	117
3.4.3.3. AFM microscopy.....	118
3.4.3.4. SEM microscopy.....	121
Conclusions.....	123
References.....	124
4. Obtaining of forsterite ceramics.....	129
4.1. Ceramics obtained from powder synthesis of colloidal silica.....	130
4.1.1. X-ray diffraction	130
4.1.2. Linear shrinkage of ceramics.....	132
4.1.3. Compactness characteristics of ceramics.....	133
Conclusions.....	135
4.2. Comparative study between ceramics obtained from powder with	136

TEOS precursor (sol-gel) and ceramics with talc precursor (solid state reaction method)	
4.2.1. X-ray diffraction	136
4.2.2. FTIR spectroscopy.....	138
4.2.3. AFM microscopy.....	138
4.2.4. Linear shrinkage of ceramics.....	139
4.2.5. Compactness characteristics of ceramics.....	141
4.2.6. Mineralization of forsterite ceramics with calcium phosphate...	144
4.2.7. In vitro bioactivity evaluation.....	146
4.2.7.1. X-ray diffraction	146
4.2.7.2. FTIR spectroscopy.....	149
4.2.7.3. Electronic microscopy SEM +EDS	150
4.2.7.4. AFM microscopy.....	152
4.2.8. Biocompatibility evaluation of forsterite ceramics.....	155
4.2.9. Mechanical properties determined by nanoindentation.....	157
4.2.10. Bending strength of bulk ceramics.....	162
Conclusions.....	163
References.....	164
5. Composites based on forsterite.....	167
5.1. Forsterite – polymer composites.....	167
5.1.1. Preparation of biocomposites.....	167
5.1.2. Mechanical properties.....	168
5.1.3. SEM microscopy.....	174
5.1.4. Toxicity test.....	175
5.1.5. Biocompatibility evaluation of composites.....	179
Conclusions.....	180
5.2 Forsterite with silver.....	181
5.2.1. Experimental procedure.....	181
5.2.2. X-ray diffraction	182
5.2.3. Bioactivity evaluation of forsterite with silver.....	182
5.2.2.1. X-ray diffraction	183
5.2.2.2. Electronic microscopy SEM + EDS	184
5.2.4. Citotoxicity test.....	184
5.2.5. Investigation of forsterite with silver in cell medium by optical microscopy.....	185
Conclusions.....	186
References.....	187
6. General conclusion.....	191
7. General references.....	193
8. Dissemination of scientific results.....	215

INTRODUCTION

Nanomaterials represent a branch of nanotechnology that studies materials with 1-100nm in size.^{4, 44} Nanomaterials present remarkable properties which are fundamentally different from materials studied until now at micro and macroscopic level. Due to these properties, the interest in the industry for the production and use of nanomaterials in various products are widespread areas such as semiconductors,²⁰⁷ medicine,²⁶⁶ cosmetics and food.^{45, 58}

In the last decades, a wide range of biomaterials have been produced and tested as replacements for the bone tissue.^{134, 225} Especially bioceramic materials were investigated, due to their low production costs, simple technology of fabrication and increased compatibility with hard tissues. Thus, it is important to investigate new, higher-quality bioceramic materials with an increasingly better biocompatibility.

In the last years, Si and Mg ceramics became leader in the preparation of materials for bone implants.^{83, 93, 136, 236} Previous researches showed that silicon is an essential element in skeleton development. Carlisle (1970)³⁶ was the first one who showed that silicon is the only element localised in the active area of young bones and is involved in the first stages of bones calcifying process. Schwarz and Milne²²⁸ showed that silicon deficit in rats leads to skull deformation. Magnesium is also one of the most important elements in human body, being closely associated with mineralization of calcified tissues,¹⁶³ having a direct influence over the mineral metabolism.⁶

In oxide system MgO-SiO₂ are highlighted two important compounds, enstatite (MgSiO₃) and forsterite (Mg₂SiO₄).⁴¹

Enstatite (MgSiO₃) has different polymorphs. The stable forms at high and low temperatures are protoenstatite and orthoenstatite, respectively. A stable form, clinoenstatite, can be formed from ortho- or protoenstatite depending on temperature, internal stresses in grains, and grain size. The changes of enstatite structure under different environmental situations can cause volume changes and produce intrinsic stress, which in turn, decrease the mechanical properties of this material in medical application.²⁵⁵

On the contrary, forsterite does not have any volume changes and due to its good biocompatibility, may be used as a substitute for enstatite bioceramics.

During the synthesis of forsterite, it is very difficult to avoid the formation of enstatite (MgSiO₃) or/and MgO, and thermal treatments up to 1200-1600°C are necessary to obtain pure forsterite. The presence of enstatite in forsterite powder could be detrimental

to the high temperature properties of the material because enstatite dissociates into forsterite and a SiO₂-rich liquid at 1557°C^{65, 222}.

Since the formation of forsterite is recognized to be difficult, the purpose of this research was to develop alternative synthesis of biomaterials based on forsterite. The methods to prepare forsterite were: sol-gel, solid state reaction and precipitation. Forsterite powders characterization was done by X-ray diffraction, SEM and TEM microscopy, FT-IR spectroscopy, atomic force microscopy (AFM), thermal analysis (TG, DTA) and laser granulometry. Biocompatibility evaluation was performed by soaking forsterite powder in the simulating body fluids (SBF) and making experiments by adhesion and spreading of osteoblasts on forsterite nanopowders, ceramics and composites. Mechanical tests were performed using nanoindenter and classical method.

Keywords:

Forsterite

Nanopowders

Bioceramic

Bioactivity

Biocompatibility

Mechanical properties

Composites

ORIGINAL CONTRIBUTION

PREPARATION OF FORSTERITE

The synthesis of forsterite (Mg_2SiO_4) was achieved by reaction between various compounds of silicon and magnesium. To bring silica in the system it was used raw materials like colloidal silica, TEOS ($\text{C}_8\text{H}_{20}\text{O}_4\text{Si}$) and talc ($\text{Mg}_3\text{Si}_4\text{O}_{10}(\text{OH})_2$) and for magnesium were $\text{Mg}(\text{NO}_3)_2 \cdot 6\text{H}_2\text{O}$, $\text{MgSO}_4 \cdot 7\text{H}_2\text{O}$, $\text{MgCl}_2 \cdot 6\text{H}_2\text{O}$, MgCO_3 , MgO .

Raw materials, methods of preparation and synthesis temperatures used in experiments are presented in table 3.1.

Table 3.1. Precursors and synthesis conditions of forsterite

Precursors			Synthesis methods	Synthesis temperatures [°C]
Colloidal silica	TEOS	Talcum		
In reaction with:				
-	$\text{Mg}(\text{NO}_3)_2 \cdot 6\text{H}_2\text{O}$	-	Sol-gel	800, 900, 1000
$\text{Mg}(\text{NO}_3)_2 \cdot 6\text{H}_2\text{O}$	-	-		1100, 1200, 1300
$\text{MgSO}_4 \cdot 7\text{H}_2\text{O}$	-	-		1100, 1200, 1300
$\text{MgCl}_2 \cdot 6\text{H}_2\text{O}$	-	-		1100, 1200, 1300
MgCO_3	-	-	Solid state reaction	1100, 1200, 1300
MgO	-	-		1100, 1200, 1300
-	-	MgCO_3		1000, 1100, 1200
-	-	$\text{Mg}(\text{NO}_3)_2 \cdot 6\text{H}_2\text{O}$		1000, 1100, 1200
-	-	$\text{MgSO}_4 \cdot 7\text{H}_2\text{O}$		1000, 1100, 1200
-	$\text{Mg}(\text{NO}_3)_2 \cdot 6\text{H}_2\text{O}$	-		Precipitation

Preparation of forsterite from colloidal silica

Forsterite powders were obtained from SiO_2 and MgO , MgCO_3 , $\text{MgSO}_4 \cdot 7\text{H}_2\text{O}$, $\text{MgCl}_2 \cdot 6\text{H}_2\text{O}$ and $\text{Mg}(\text{NO}_3)_2 \cdot 6\text{H}_2\text{O}$, respectively. The methods used for preparation were solid state reactions and sol-gel methods. Samples were fired at 1100°C , 1200°C and 1300°C . In both cases, $\text{MgO}:\text{SiO}_2$ molar ratio of 2:1 was used.

Thermal analysis (DTA, TG) carried out for mixture formed from colloidal silica and MgCO_3 (Figure 3.1) shows the presence of endothermic effects and considerable weight loss especially around 400°C due to decomposition of magnesium carbonate. The process takes place at a relatively low temperature due to the very fine grain size or increase the surface area of the sample.

FT-IR spectroscopy for samples prepared at 1200°C show in all samples the presence of characteristic absorption bands for forsterite. The crystalline components of sample 3 ($\text{MgSO}_4 \cdot 7\text{H}_2\text{O}$) and 4 (MgCO_3) that were prepared at 1100°C was evidenced by X-ray diffraction. In the sample 3 MgO characteristic reflections appear. Forsterite forming reaction is incomplete due to the high temperature decomposition of MgSO_4 . In sample 4 are shown characteristic enstatite reflexes sign of incomplete reaction in this case.

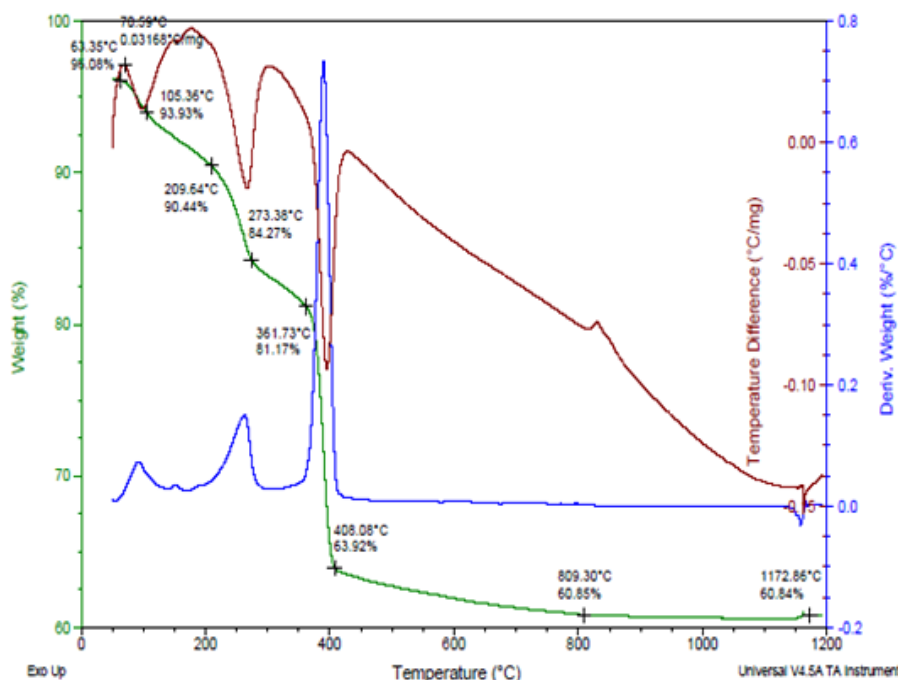


Figure 3.1. Thermal behavior of sample 4 (MgCO_3 with colloidal silica) ¹⁸

Preparation of forsterite from silica precursor, TEOS

Preparation of forsterite with sol-gel method from $\text{Mg}(\text{NO}_3)_2 \cdot 6\text{H}_2\text{O}$, TEOS and additives

In order to synthesize the forsterite powder, it was used hexahydrated magnesium nitrate ($\text{Mg}(\text{NO}_3)_2 \cdot 6\text{H}_2\text{O}$) and tetraethyl orthosilicate (TEOS- $\text{C}_8\text{H}_{20}\text{O}_4\text{Si}$, Merck) as raw materials, and polyvinyl alcohol (PVA), sucrose and nitric acid as binder and pH regulators.

The synthesis was performed at temperatures of 800, 900 and 1000°C (figure 3.10). The patterns show that the sample fired at 800°C has a lower crystallinity degree, the pattern being dominated by the peaks of periclase, MgO. The increase of temperature is accompanied by the formation of well-crystallized forsterite (figure 3.11). Periclase is also present in the sample obtained at 1000 °C; nevertheless, enstatite peaks were not identified (probably their intensities being below the equipment's limit of detection).

The grain size distribution has shown that the powder is nanometre-in size in the case of the lower temperatures, in most cases below 40 nm (figure 3.12). In the case of the sample synthesised at 1000°C, the sizes increased due to particle agglomeration at higher temperatures.

The *in vitro* bioactivity test has proven that the forsterite nanopowder is highly reactive and biocompatible; thus, it can be used as bioactive material in bone reconstruction. The FTIR spectroscopy (figure 3.20), XRD and SEM+EDS analyses confirmed the formation of hydroxyapatite on the nanoforsterite samples starting with the 7th day of immersion into the SBF solution.

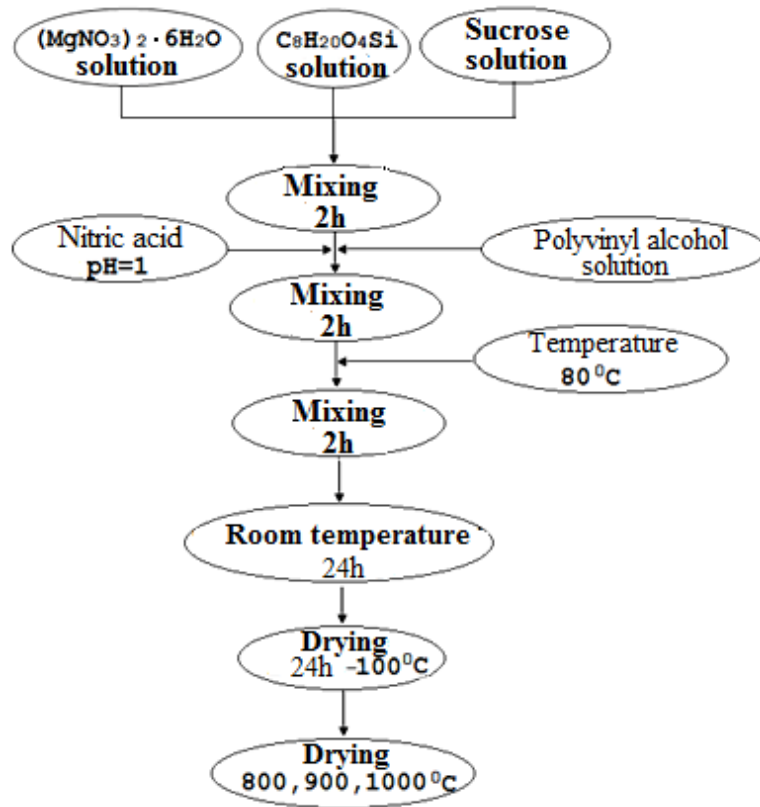


Figure 3.10. Schematic flow chart of forsterite synthesis by sol-gel method and additives

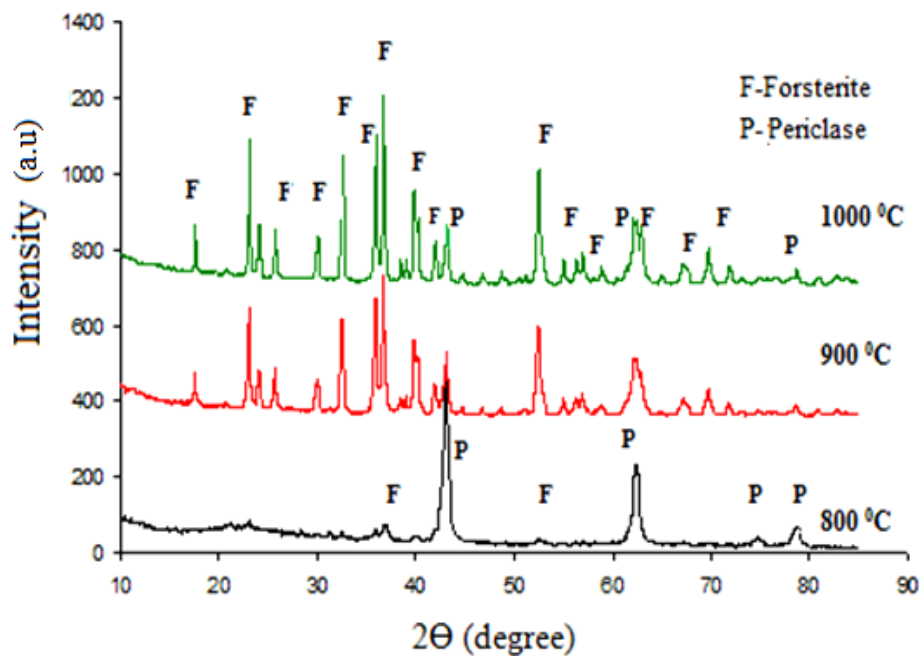


Figure 3.11. X-ray diffraction for the forsterite synthesized at various temperatures ¹⁸⁵

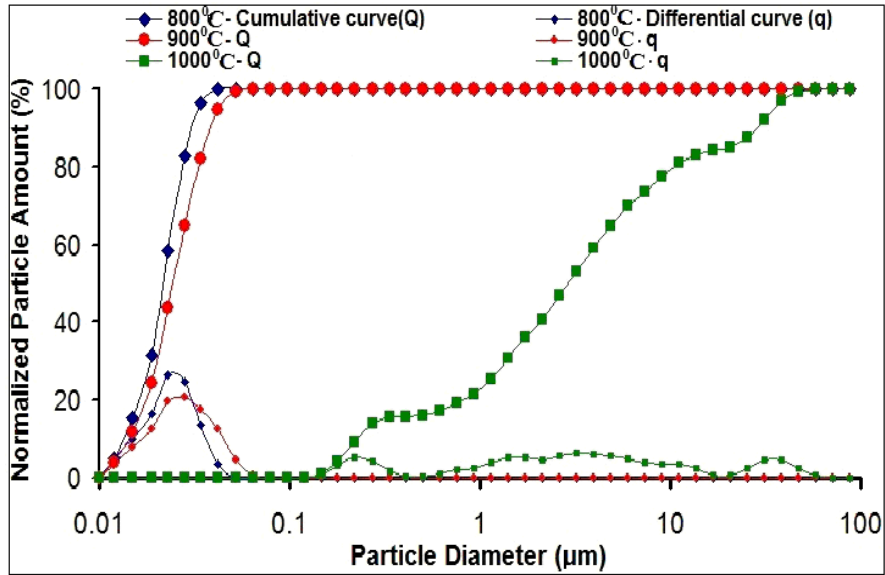


Figure 3.12. Grain size distribution for the forsterite nanopowders synthesized at various temperatures¹⁸⁵

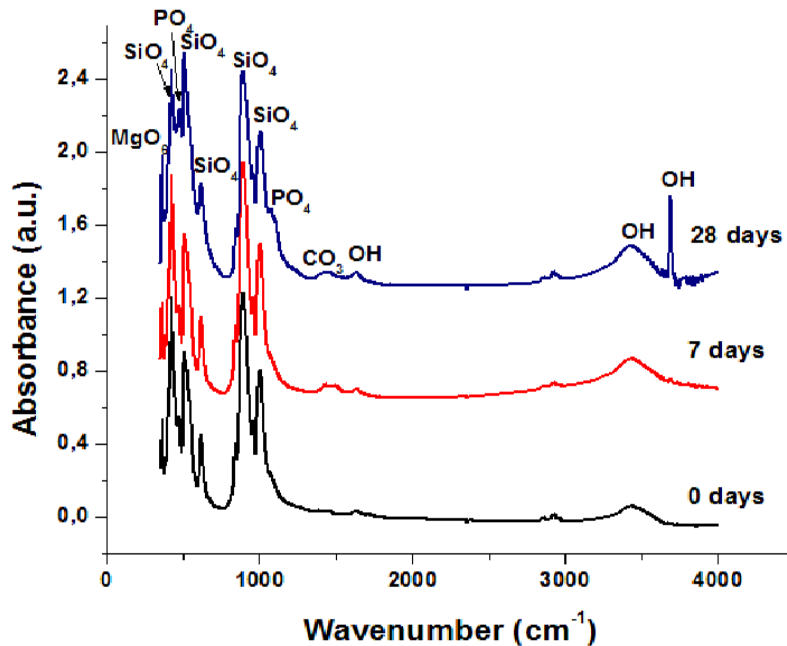


Figure 3.20. FTIR spectroscopy of the forsterite powder fired at 900°C placed in a SBF solution for various periods of time¹⁸⁵

The MTT test (figure 3.25) has shown that the osteoblast's spreading rate increases with the cultivation time, in the absence of any cytotoxicity signs. These results show that the forsterite nanopowder obtained by using the method applied in this study represents a

biocompatible material that allows that formation of HAP during its immersion into SBF solution.

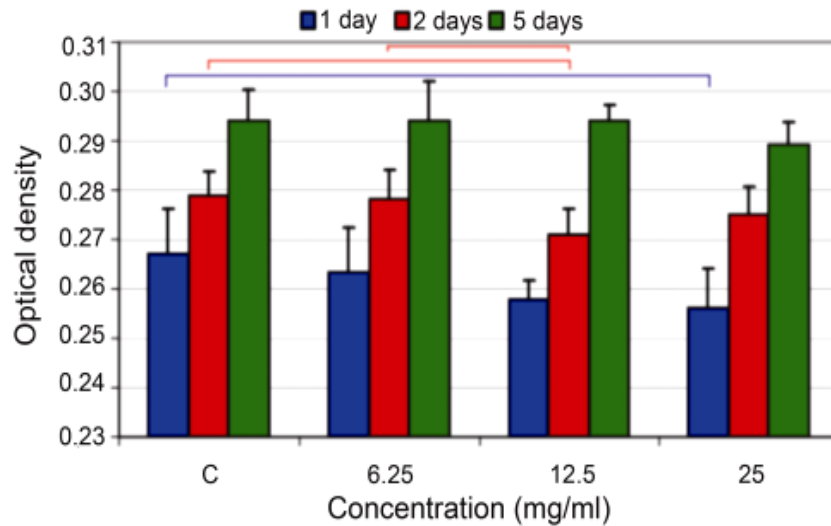


Figure 3.25. Results of the MTT test performed on forsterite powders in different concentrations, after different intervals of cell culture using U2OS-type osteoblast cells. Data are presented as mean values; they were considered as statistically significant at $p < 0.05$ difference in the same day when compared using the Tukey test

The results show that forsterite nanopowder is a biocompatible material and allow the formation of HAP by maintaining the powder in SBF solution.

Preparation of forsterite by sol-gel method from $Mg(NO_3)_2 \cdot 6H_2O$ and TEOS with no additive

The preparation method is similar with previously one used from TEOS and magnesium nitrate, but in this case sugar and polyvinyl alcohol were not used as additives. The powder was calcined at 900°C.

Thermal analysis performed on the gel obtained after synthesis, dried at 100°C (Figure 3.28, 3.29) illustrates the thermal effects and weight losses during heat treatment represented by DTA and TG curves.

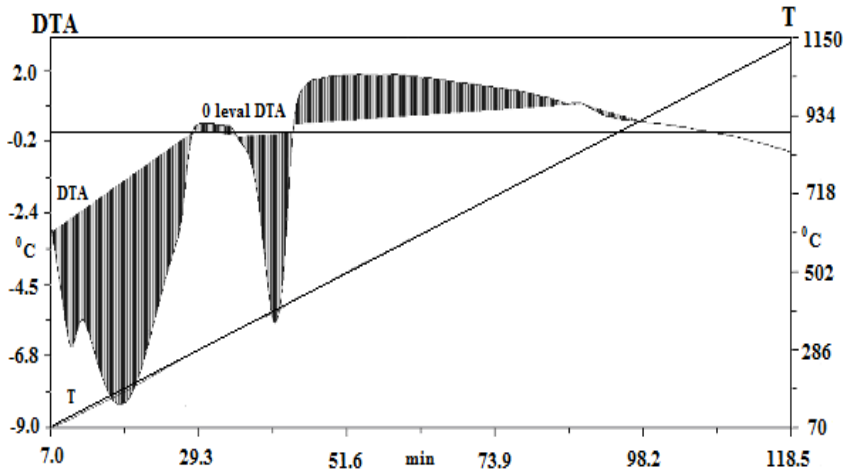


Figure 3.28. Differential thermal analysis of the dried gel at 100°C

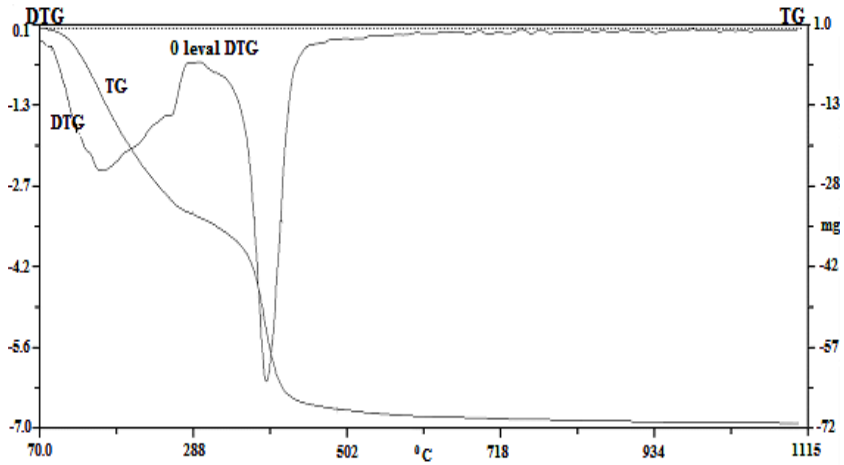


Figure 3.29. Thermogravimetric analysis of the dried gel at 100°C

According to the particle size distribution of the forsterite powder, the grain size is in the range 10 to 23 nm (65%) and the maximum size is 42 nm.

Preparation of forsterite by precipitation method from $\text{Mg}(\text{NO}_3)_2 \cdot 6\text{H}_2\text{O}$ and TEOS

Nanocrystalline forsterite (Mg_2SiO_4) was synthesized by precipitation method from hexahydrated magnesium nitrate ($\text{Mg}(\text{NO}_3)_2 \cdot 6\text{H}_2\text{O}$), tetraethyl orthosilicate (TEOS) and sodium hydroxide as pH regulators. The crystallite size of the powder calcined at 900°C is in the range 19-25 nm and the particle size is smaller than 45 nm. This chemical synthesis without sucrose and PVA is applicable and produces nanocrystalline forsterite powder with characteristics compared to those of other processes of preparing. The crystallization

temperature of forsterite is about 800 °C according to the thermal analyses data (figure 3.35).

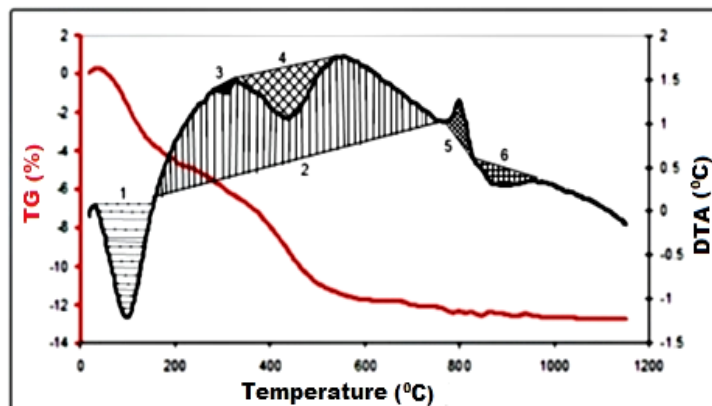


Figure 3.35. DTA and TG curves for dried powder¹⁸⁴

The obtained powder has uniform sized particles with a weak agglomeration of particles according to particle size analysis.

Preparation of forsterite by solid state reaction method from talc

Forsterite powder was synthesized by solid-phase reaction method from talc ($\text{Mg}_3\text{Si}_4\text{O}_{10}(\text{OH})_2$) and different magnesium salts. The mixture of materials was milled for 10 hours until were obtained a powder than heat treated at different temperatures.

Preparation of forsterite from MgCO_3 and talc

The forsterite powder was prepared by using the solid state reaction method starting from magnesium carbonate and talc, followed by thermal treatment at 1000, 1100 and 1200°C. As proven by the X-ray diffraction patterns (figure 3.43), the reaction of formation of the forsterite nanopowder is completed after mechanical activation for 10 hours and firing at 1100°C. TEM and SEM microscopy evidence the formation of nanocrystallites of irregular shapes that sometimes form aggregates.

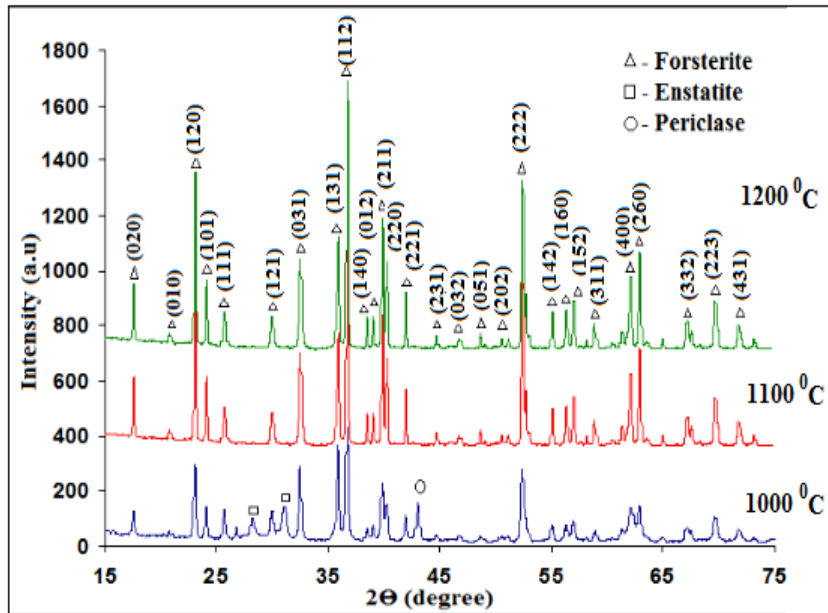
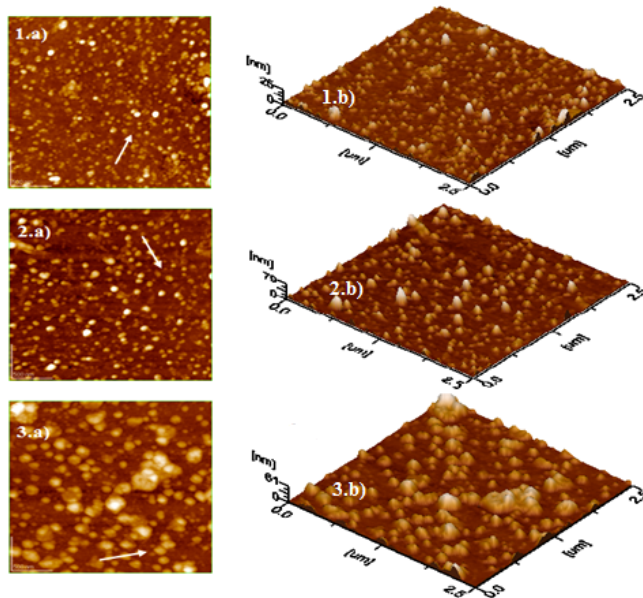


Figure 3.43. X-ray diffraction patterns on the experimental samples ⁹⁷

The AFM analysis (figure 3.45) confirms the nanometre-size range of the crystallites for the powders fired at 1000°C and respectively 1100°C, and illustrates the formation of thin films with the rough surfaces.



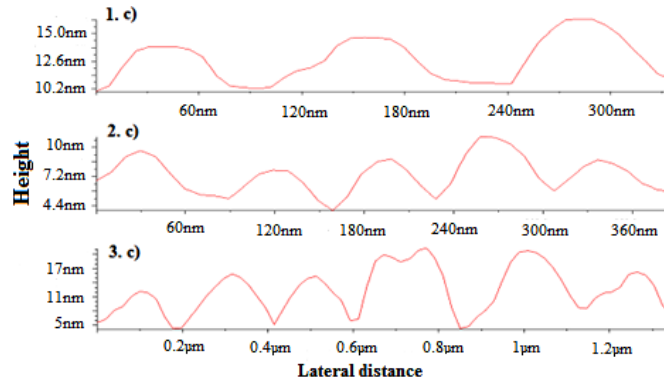


Figure 3.45. AFM images of the forsterite powder fired at 1) 1000°C; 2) 1100°C; and 3) 1200°C. Measured panel: 2.5 μm x 2.5 μm. a) 2D-topography; b) 3D-images of the panels c) cross section along the arrow in panels a) ⁹⁷

The investigation of the grain size distribution (by Coulter Counter granulometer) indicated nanometre-sized forsterite grains in the sample fired at 1000 and 1100°C, with most of the grains below 40 nm in size. Grain sizes are larger, micrometer in size, in the case of the sample synthesized at 1200°C mainly as a result of grain aggregation processes.

TEM (Figure 3.46) and SEM (3.48) microscopy show the formation of nano-sized crystallites and the presence of irregularly shaped clusters of crystallites.

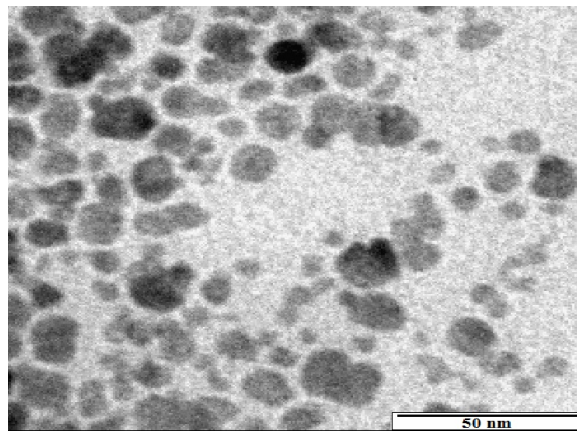


Figure 3.46. TEM image of the powder synthesized at 1100°C ⁹⁷

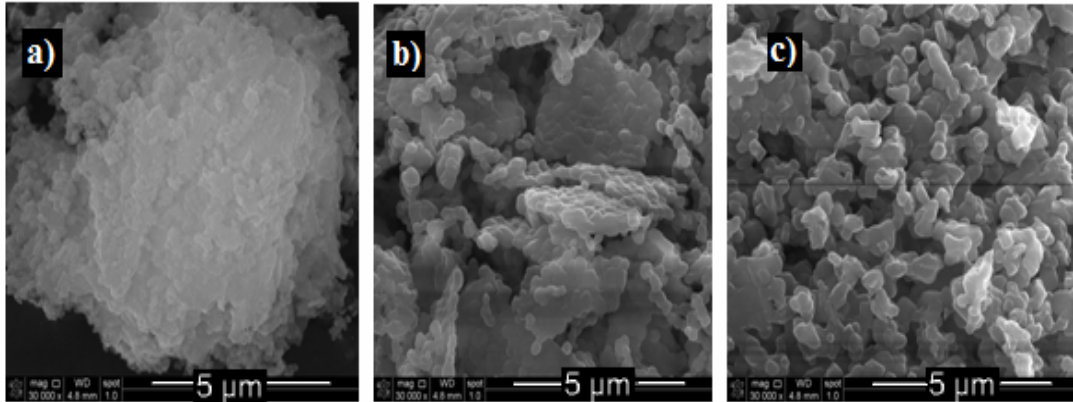


Figure 3.48. SEM images on the forsterite powders fired at 1000, 1100 and respectively 1200°C⁹⁷

The FTIR spectroscopy results clearly demonstrate the formation of hydroxylapatite on the nanometre-sized forsterite grains after 28 days of immersion in the SBF fluid. At the same time, this process is less evident in the case of the larger, micrometre-sized powders (figure 3.49). The *in vitro* bioactivity tests show a good bioactivity reaction for the synthesized forsterite nanopowders. So, nano forsterite can be successfully used as biomaterials in the remediation of bone tissue.

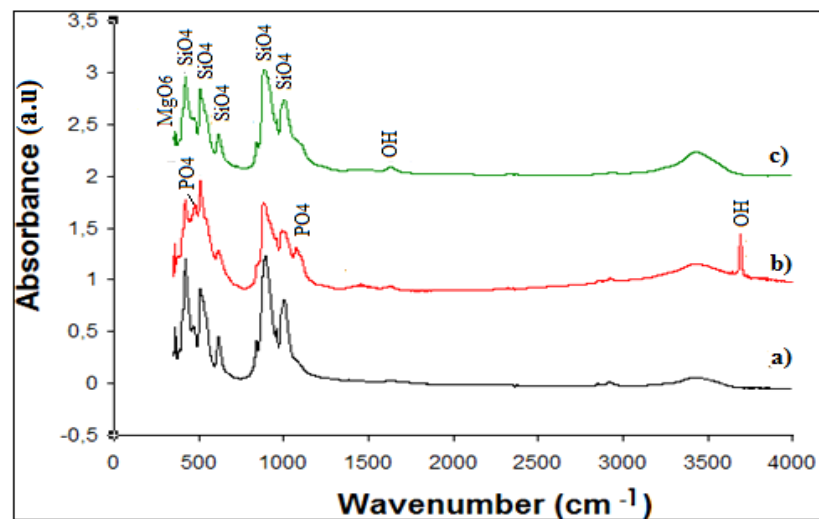


Figure 3.49. FTIR spectra of the forsterite powders: a) sample fired at 1100°C, before immersion in SBF; b) and c) sample fired at 1100°C and 1200°C respectively and immersed in the SBF fluid for 28 days

Preparation of forsterite from $\text{Mg}(\text{NO}_3)_2 \cdot 6\text{H}_2\text{O}$ and talc

Forsterite powder was prepared by solid state reaction from magnesium nitrate and talc, heat-treated at temperatures of 1000, 1100 and 1200°C. X-ray diffraction shows that the main component is forsterite at the temperature of 1200°C. Also, the sample is containing a small amount of periclase and enstatite. This suggests that the reaction was not completed probably due to insufficient mixing of raw materials and possibly of low temperature of synthesis.

SEM microscopy shows the formation of nano and micrometer-sized crystallites and the presence of clusters of crystallites. AFM analysis confirms the nanometric size of the crystallites for powder calcined at 1100°C and micron sizes for powders treated to other temperatures. Coulter Counter particle size distribution analysis shows that nanosized forsterite is obtained for samples calcined at 1100°C. In the case of the sample treated at 1200°C, particle size increases and agglomeration of the particles occurs, leading to micron size granules.

Preparation of forsterite from $\text{MgSO}_4 \cdot 7\text{H}_2\text{O}$ and talc

Forsterite was prepared by solid state reaction from magnesium carbonate and talc. Calcinations temperatures were 1000, 1100 and 1200°C. X-ray diffraction analysis shows the reaction was not completed and a small amount of forsterite was obtained at 1000°C. At 1200°C the crystallinity of forsterite increases, but is still present a significant amount of enstatite and periclase. SEM microscopy shows the formation of nano and micrometer-sized crystallites and the presence of clusters of crystallites. AFM, SEM and Coulter Counter analysis of particle size distribution confirms the nanometric size of the crystallites for powder burned at 1000°C and micrometer dimensions for powders treated to other annealing temperatures. The AFM and SEM analysis show an increase in size and an agglomeration of the particles.

OBTAINING OF FORSTERITE CERAMICS

Ceramics from powder synthesis of colloidal silica

Porous ceramics based on forsterite was sintered at 1350°C from powders obtained by solid state reaction and sol-gel methods using various reactants. Common reagent for each mixture was colloidal SiO₂. To bring magnesium in the system the MgO, Mg(NO₃)₂·6H₂O, MgSO₄·7H₂O, MgCl₂·6H₂O, MgCO₃ were used.

For using as biomaterial the forsterite ceramics must to have a particular porosity. Porous ceramics were obtained with different porosity values, depending on the initial reactants and the temperature of sintering. Ceramics have been characterized in terms of the firing shrinkage (Table 4.1) and compactness.

Tabel 4.1. Ceramics shrinkage at 1350°C

Sample number	Ceramics sintered at 1350°C shrinkage [%] from		
	powder synthesized at temperature of		
	1100°C	1200°C	1300°C
1	8.51	5.00	4.50
2	21.87	15.76	4.50
3	1.48	1.13	0.63
4	15.55	14.42	7.11
5	8.86	6.19	3.37

Mineralogical characterization was performed by X-ray diffraction for ceramics obtained at 1350°C from powders synthesized at 1100°C. Result shows that forsterite is majority crystalline phase in the fired ceramic sintered at 1350°C.

The natural bones have high porosity inside and are more compact to the outside. A possible option would be to realize bioceramics implants with porosity imitating bones structure. The forsterite ceramics have better mechanical properties and improve the regeneration of bone than other ceramics.²⁸⁴

In conclusion, if it is desired a higher apparent porosity than 40% with low firing shrinkage (0.5-2%), a possible way is the synthesis of forsterite by sol-gel method from

$\text{MgSO}_4 \cdot 7\text{H}_2\text{O}$ and SiO_2 at 1100°C . For obtaining the forsterite ceramics the powders have to sinter at 1350°C .

Comparative study between ceramic obtained from powder with TEOS precursor (sol-gel) and ceramic with talc precursor (solid state reaction method)

Ceramics were prepared starting from forsterite powder obtained by sol-gel method (SG) and solid state reaction (FS). Sintering temperatures were $1200 - 1450^\circ\text{C}$.

X-ray diffraction confirms that formation of forsterite is complete in the case of ceramic FS. AFM analysis shows that particles size increases until micro dimension by sintering the powders and obtaining the ceramics (figure 4.6.)

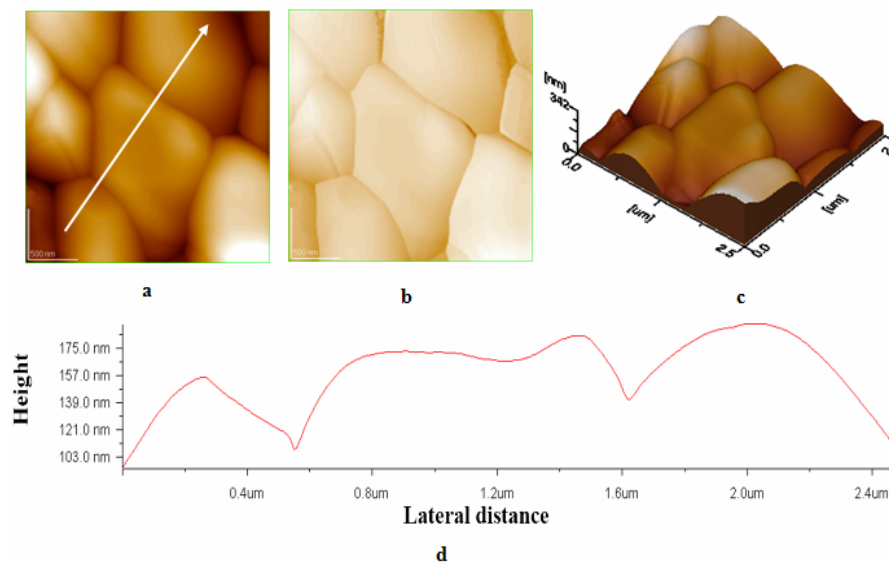


Figure 4.6. AFM images of SG ceramic sintered at 1400°C . Scanning area: $2.5\mu\text{m}/2.5\mu\text{m}$. a) 2D-topography b) phase image c) 3D image d) cross-section along the arrow in panel a)

SG ceramic shrinkage does not increase significantly, keeping close values between 1200 and 1450°C . FS ceramic shrinkage is small at the temperature of 1200°C , but is significantly increased at temperature of 1300°C and then the values are keeping closed at temperature of 1450°C .

Apparent porosity (Figure 4.9) of FS ceramics sintered at 1200°C is higher than SG ceramic sintered at the same temperature. With increasing sintering temperature the porosity of FS ceramic is significantly decreased compared with SG.

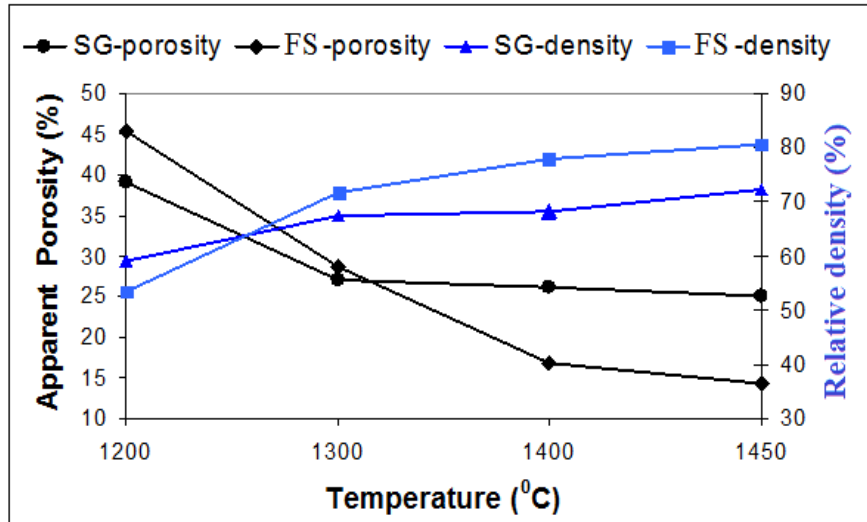


Figure 4.9. Apparent porosity and relative density of SG and FS ceramics sintered at different temperatures

FTIR, XRD and SEM with EDS analysis (Figure 4.20) confirm the formation of hydroxyapatite on ceramics after different intervals of maintaining in SBF solution, most convincing at 3 months.

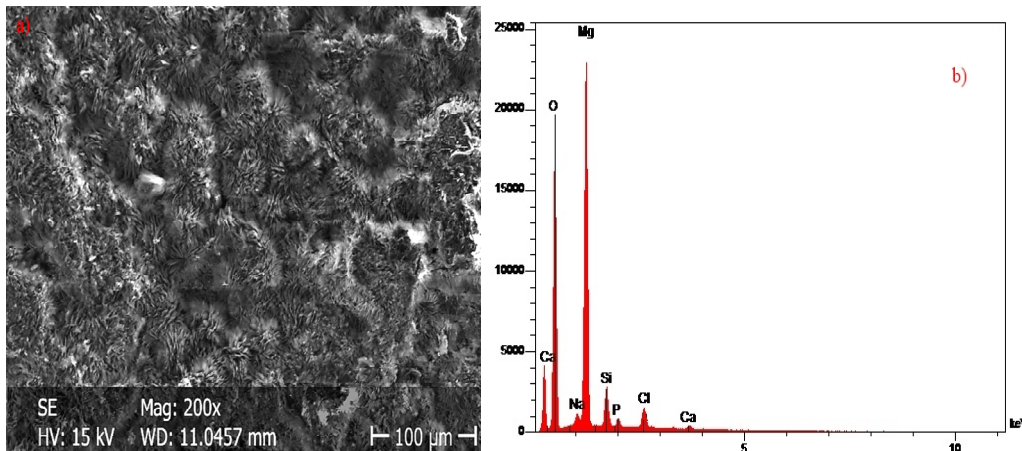


Figure 4.20. SG ceramics sintered at 1200°C after 3 months of keeping sample in SBF. a) SEM image, b) EDS spectrum

MTT assay (Figure 4.24) confirms that the rate of spreading fibroblast cells is increased with increasing time of cultivation on the ceramic surface without significant toxicity effect.

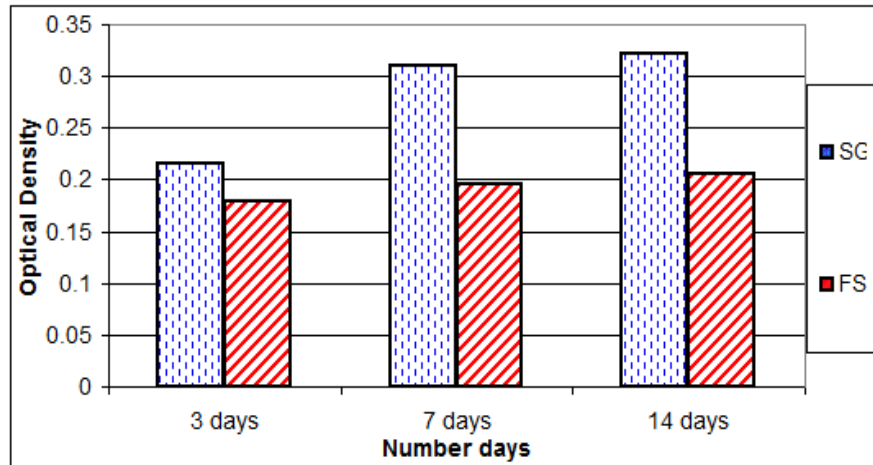


Figura 4.24 MTT test realised on SG and FS ceramics

The maximum values of hardness and elastic modulus of forsterite ceramics are 101.34 GPa and 8.19 GPa respectively. These values are better than those obtained on pure hydroxyapatite.

Forsterite ceramics possess good bioactivity, biocompatibility and mechanical strength and can be used as a biomaterial for repairs and bone implants.

COMPOSITES BASED ON FORSTERITE

Forsterite-polymers composites

Forsterite powder was prepared from magnesium nitrate and TEOS with sol-gel method. Calcination temperature was 900°C. The polymer matrix was obtained by mixing the monomer Bis-GMA (60% by weight) and TEGDMA (40% by weight).

In order to improve the biological and mechanical properties of the polymer the composites were prepared by adding the forsterite nanopowder of 5, 15, 30, 50 and 70% by weight into polymer (Table 5.1).

Tabel 5.1. Composition of the composite (ratio between polymer – forsterite)

Code	Filler amount [%] Forsterite (F)	Polymer amount [%] L	F/L [%]
C0	-	100	0/100
C5F	5	95	5/95
C15F	15	85	15/85
C30F	30	70	30/70
C50F	50	50	50/50
C70F	70	30	70/30

The results show that compressive strength, bending strength (figure 5.2) and diametral tensile strength increase with increasing the amount of filler (forsterite) until 50%. Compressive and flexural modulus values (figure 5.3) increase up until the filler content reach 70% by weight.

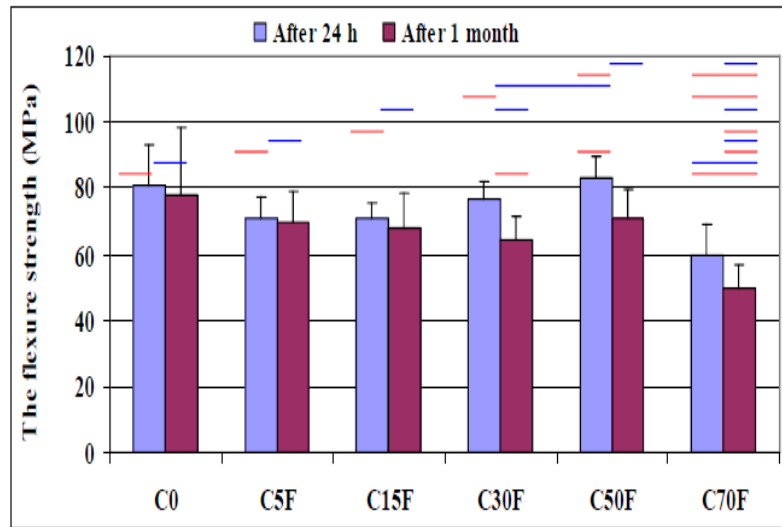


Figure 5.2. The flexural strength of composites. (The horizontal bar indicates the average values were statistically significant different, compared with Tukey test $P < 0.05$)

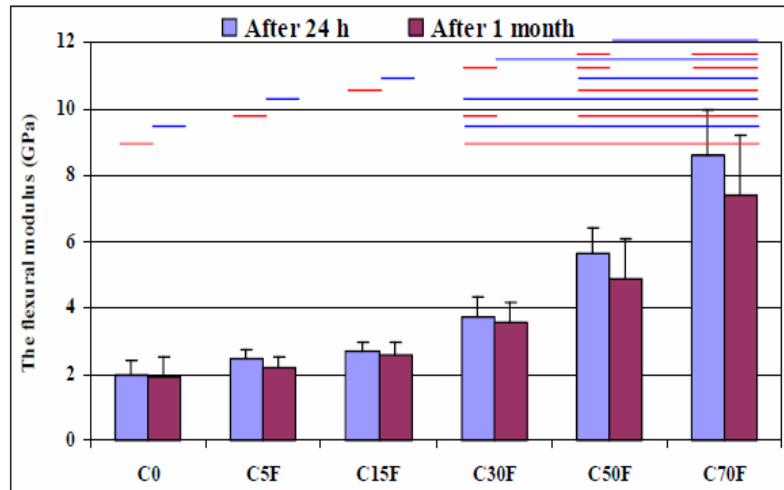


Figure 5.3. Flexural modulus of composites obtained from forsterite and polymer. (The horizontal bar indicates the average values were statistically significant different, compared with Tukey test $P < 0.05$)

SEM with EDS microscopy (Figure 5.10) confirm the biomineralization of composites. The biological tests show an improved cell adhesion with increasing amount of forsterite.

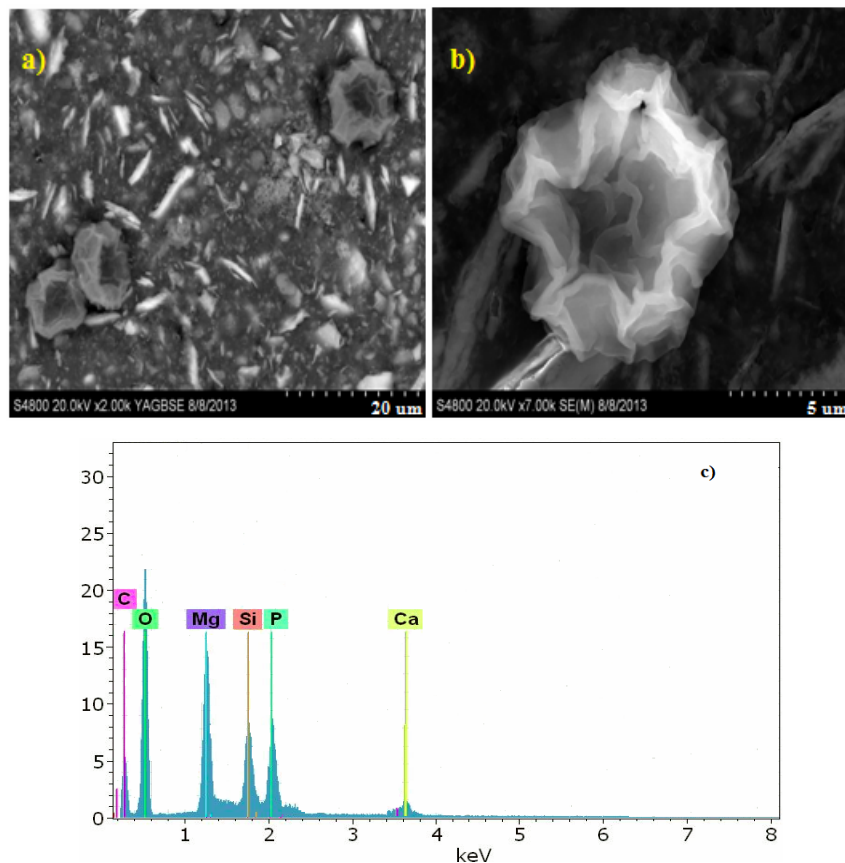


Figure 5.10. a) and b) SEM images, c) EDS spectrum on surface (b) of composite C50F after immersion in SBF solution for 28 days

C50F composite can be used as bone or dental implant in various biomedical applications.

Forsterite with silver addition

10% silver was added to forsterite nanopowders. X-ray diffraction shows that forsterite with silver composite contains periclas and enstatite due to an incomplete reaction.

The obtained results after testing bioactivity of forsterite with silver addition maintained in SBF solution show formation of HAP; the formed amount of HAP is lower than in pure forsterite.

MTT assay shows that the rate of cells spread on different concentrations of forsterite dilution, increases with increasing cultivation time at all concentrations but decreases with increasing concentration of silver.

GENERAL CONCLUSION

Forsterite (Mg_2SiO_4) was synthesized by three methods (sol-gel, solid state reaction and precipitation) using precursors of magnesium ($(Mg(NO_3)_2 \cdot 6H_2O)$, $MgSO_4 \cdot 7H_2O$, $MgCl_2 \cdot 6H_2O$, $MgCO_3$, or MgO), and silicon precursors (TEOS, colloidal silica and talc).

With the help of thermal analysis it was established the changes that take place during heat treatment in order to determine the optimal temperature for the synthesis. X-ray diffraction shows that the best results were obtained for forsterite prepared by sol-gel method from TEOS and magnesium nitrate, by precipitation method from magnesium nitrate and TEOS or solid state reaction from magnesium carbonate and talc.

SEM, TEM and AFM microscopy have revealed the shape and particle size in order to determine the optimal synthesis temperature for powder to obtain nanosized powders.

Powder bioactivity was investigated by immersion in simulated body fluid (SBF). It was found that formation of hydroxyapatite on forsterite nanopowders starts at 7 days and is well developed at 28 days.

Biocompatibility of the material was investigated by MTT assay using human osteoblast cells. The MTT assay demonstrates that powder of forsterite is not toxic to cells and, therefore, can be used as biomaterial for medical applications.

Ceramics were prepared by dry method from forsterite powder prepared by sol-gel (SG) and solid state reaction (FS). The samples were dried pressed and fired at temperatures of 1200- 1450°C.

Ceramics have been characterized from the point of view of compactness and firing shrinkage. Porous ceramics were obtained with different porosity values, depending on the initial reactants and the sintering temperature. The porosity of ceramics can be achieved according to the requirement of the use and correlated with the mechanical strength.

FTIR, XRD and SEM with EDS analysis confirm the bioactivity of forsterite ceramics. Hydroxyapatite was formed after maintaining ceramics in SBF solution, the most obvious deposits are recorded at 3 months.

MTT assay demonstrated that the rate of spreading fibroblast cells increases with increasing time of cultivation on the ceramic surface without significant toxicity effect. Best behavior in culture medium had SG ceramic.

The maximum values of hardness and elastic modulus of forsterite ceramics are 101.34 GPa, 8.19 GPa respectively, values higher than those obtained on pure hydroxyapatite (2.81 GPa, 45.33 GPa respectively). Best mechanical strength presents FS ceramics.

Forsterite ceramics possess good bioactivity, biocompatibility and mechanical strength therefore can be used as biomaterial for repairs and bone implants.

Preparation of polymer matrix composite with forsterite powder filler is intended for use in dentistry.

SEM / EDS microscopy confirm the composites biomineralization. Biological tests show an increased cell adhesion with increasing amount of forsterite.

Increasing the amount of forsterite improves the mechanical resistance of the composite. Composite with 50% forsterite filler has the best properties in terms of mechanical resistance and biocompatibility. This composite can be used as bone or dental implant in various biomedical applications.

Forsterite with silver is intended for medical applications due to the antimicrobial activity of silver.

After testing the biocompatibility of this material was found that there is an optimum value for silver to develop antimicrobial properties. A high Ag content can be toxic to the human body.

In conclusion, it is evident that forsterite nanopowder can be synthesized from various precursors of silicon and magnesium at synthesis temperatures between 900 and

1100°C. Forsterite powders, ceramics and composites are biocompatible and bioactive. Compressive and bending resistance of forsterite ceramics is higher than hydroxyapatite ceramics resistance. So, the forsterite ceramics could be recommended in medical applications as a substitute for human bone.

Selective bibliography

4. Ali Kermanizadeh, Sandra Vranic, Sonja Boland, Kevin Moreau, Armelle Baeza-Squiban, Birgit K Gaiser, Livia A Andrzejczuk and Vicki Stone, An in vitro assessment of panel of engineered nanomaterials using a human renal cell line: cytotoxicity, pro-inflammatory response, oxidative stress and genotoxicity, Kermanizadeh et al. BMC Nephrology, 14:96, 2013.
6. Althoff, J., Quint, P., Krefting, E.R., Hohling H.J., Morphological studies on the epiphyseal growth plate combined with biochemiacal and X-ray microprobe analysis, Histochemistry, 74, 541–552, 1982.
36. Carlisle, E.M., Silicon: a possible factor in bone calcification, Science, 167, 279–280, 1970.
41. Budnicov P.P., Berejnoi A.S., Bulavin I.A., Cucolev G.V., Perevalov V.I., Smelianschi I.S., Tehnologia produselor ceramice, Ed.Tehnică, 140-141, 1951.
44. Buzea C, Pacheco II, Robbie K: Nanomaterials and nanoparticles: sources and toxicity. Biointerpahses, 2:18–67, 2007.
45. Calzolari L, Gilliland D and Rossi F, Measuring nanoparticles size distribution in food and consumer products: a review Food Addit Contam A, 2012.
58. Dekkers S, Krystek P, Peters R J B, Lankveld D P K, Bokkers B G H, van Hoeven Arentzen PH, Bouwmeester H and Oomen A G, Presence and risks of nanosilica in food products, Nanotoxicology, 5, 393-405, 2011.
65. Douy A, Aqueous Syntheses of Forsterite (Mg_2SiO_4) and Enstatite ($MgSiO_3$), Journal of Sol-Gel Science and Technology 24, 221–228, 2002
83. Fathi M. H., Kharaziha M., Mechanochemical synthesis and characterization of nanostructure forsterite bioceramics, International Journal of Modern Physics B, vol.22, Nos.18-19, 2008.

93. Ghomi H., Jaberzadeh M., Fathi M.H., Novel fabrication of forsterite scaffold with improved mechanical properties, *Journal of Alloys and Compounds*, 509, L63–L68, 2011.
97. Gorea M., **Naghiu M.A.**, Tomoaia-Cotisel M., Borodi G., Nano and microstructure effects on the bioactivity of forsterite powders, *Ceramics – Silikáty* 57 (2), pp. 87-91, 2013.
134. Kent J.N., Quinn J.H., Zide M.F., Figer I.M., Jarcho M., Rothstein S.S., Correction of alveolar ridge deficiencies with non-resorbable hydroxyapatite, *J. Am. Dent. Assoc.* 105, 993–1001, 1982.
136. Kharaziha, M., Fathi, M.H., Improvement of mechanical properties and biocompatibility of forsterite bioceramic addressed to bone tissue engineering materials, *Journal of mechanical behavior of biomedical materials* 3, 530 ±537, 2010.
163. LeGeros, R.Z., *Calcium Phosphates in Oral Biology and Medicine*, Basel, Switzerland, 1991.
183. **Naghiu M.A.**, Gorea M., Ungvary D., Tomoaia-Cotisel M., Preparation and characterization of some ceramics based on Forsterite, *Zilele Academiei de Științe Tehnice din România Ediția a VI-a, Timisoara 22-23 septembrie*, 2011.
184. **Naghiu M.A.**, Gorea M., Kristaly F., Tomoaia-Cotisel M., A new method for synthesis of forsterite nanomaterials for bioimplants, *Studia UBB Chemia*, 2013, under review.
185. **Naghiu M.A.**, Gorea M., Mutch E., Kristaly F., Tomoaia-Cotisel M., Forsterite Nanopowder: Structural Characterization and Biocompatibility Evaluation, *Journal of Materials Science & Technology*, 29, 7, 2013.
188. Napierska D, Thomassen L C, Lison D, Martens J A and Hoet P H, The nanosilica hazard: another variable entity, *Part Fibre Toxicol*, 7, 2012.
207. Piccione B, Cho C-H, van Vugt L K and Agarwal R, All-optical active switching in individual semiconductor nanowires *Nat Nano*, 7, 640-645, 2012.
222. Sanosha K.P., Balakrishnana A., Francisc L., Kima T.N., Sol–gel synthesis of forsterite nanopowders with narrow particle size distribution, *Journal of Alloys and Compounds*, 495, 113–115, 2010.
225. Scheer P., Boyne P.J., Maintenance of alveolar bone through implantation of bone graft substitutes in tooth extraction sockets, *J. Am. Dent. Assoc.*, 114, 594–597, 1987.

228. Schwarz, K., Milne, D.B., Growth-promoting effects of silicon in rats, *Nature* 239, 333–334, 1972.
236. Siyu, N., Lee, C., Jiang, C., Preparation and characterization of forsterite (Mg_2SiO_4) bioceramic, *Ceramics International* 33, 83–88, 2007.
255. Tavangarian F., Emadi R., Nanostructure effects on the bioactivity of forsterite bioceramic, *Materials Letters* 65, 740–743, 2011.
266. Wang W, Zhang S, Chinwangso P, Advincula R C and Lee T R, Electric potential stability and ionic permeability of SAMs on gold derived from bidentate and tridentate chelating alkanethiols *J Phys Chem C*, 113, 3717-3725, 2009.
284. Zhang F., Chang J., Lu J., Lin K., Ning C., Bioinspired structure of bioceramics for bone regeneration in load-bearing sites, *Acta Biomaterialia* 3, Published by Elsevier, 2007.

COMMUNICATIONS:

- 1. International conference:** NAGHIU M.A., GOREA M, UNGVARI D.M, TOMOAI A-COTISEL M, Preparation and characterization of some ceramics based on Forsterite, Academic Days of Tehnic Science from Romania, Edition VI,, Timisoara 22-23, september 2011
- 2. International conference:** NAGHIU M.A., GOREA M, UNGVARI D.M, TOMOAI A-COTISEL M, Preparation, characterization and medical applications of some ceramics based on forsterite, COST Action TD0903: The 3rd Workshop and 4th Management meeting Understanding and Manipulating Enzymatic and Proteomic Processes in Biomineralization, Cluj Napoca, Romania, 11th – 13th October, 2011
- 3. International conference:** NAGHIU M.A., GOREA M, TOMOAI A-COTISEL M, Synthesis and characterization of forsterite nanopowder obtained by sol-gel method, 8th International Conference of PhD students, university of Miskolc, Hungary, 5-11 August, 2012
- 4. National conferecnce:** NAGHIU M.A., GOREA M, TOMOAI A G., FURTOS G, MOCANU A, TOMOAI A-COTISEL M., Synthesis and characterization of nano forsterite, 32 national conference, Calimanesti, 3-5 october 2012
- 5. International conference:** NAGHIU M.A., GOREA M, TOMOAI A-COTISEL M, FRANKEL D, Study of mechanical properties of forsterite ceramics using nanoindentation method, COST Action TD0906, WG3 & WG4 Scientific Workshop Biological Adhesives: from Biology to Biomimetics, Cluj Napoca, Romania, 9 -11 of April 2013
- 6. International conference:** FURTOS G, NAGHIU MA., DECLERCQ H, CORNELISSEN M, GOREA M, TOMOAI A-COTISEL M, PREJMEREAN C, Nano forsterite biocomposites for biomedical application: Mechanical properties

and bioactivity, The 4th International Symposium on Surface and Interface Biomaterials, Roma, Italy, 24-28, September 2013

LIST OF PUBLICATIONS:

1. **NAGHIU M.A.**, GOREA M, UNGVARI D.M, TOMOAI-COTISEL M,, Preparation and Characterization of some ceramics based on forsterite, Vol. Proceedings of VI-th International Conference Academic Days of Tehnic Science from Romania, Ed. Agir, ISSN 2066 – 6586, 298-303, September 2011.
2. **NAGHIU M.A.**, GOREA M, TOMOAI-COTISEL M, Synthesis and characterization of forsterite nanopowder obtained by sol-gel method, Proceedings: 8th International Conference of PhD students, University of Miskolc, Hungary, 5-11 August, 2012.
3. **NAGHIU M.A.**, GOREA M, MUTCH E, KRISTALY F, TOMOAI-COTISEL M, Forsterite nanopowder: Structural characterization and biocompatibility evaluation, Journal of Materials Science and Technology 29 (7), pp. 628-632, 2013.
4. GOREA M, **NAGHIU M.A.** TOMOAI-COTISEL M, BORODI G, Nano and microstructure effects on the bioactivity of forsterite powders, Ceramics – Silikáty 57 (2), pp. 87-91, 2013.
5. **NAGHIU M.A.**, GOREA M, KRISTALY F, TOMOAI-COTISEL M, A new method for synthesis of forsterite nanomaterials for bioimplants, Studia UBB Chemia, 2013, under review.